Int J Adv Manuf Technol (2011) 57:957–967
DOI 10.1007/s00170-011-3361-z

ORIGINAL ARTICLE

A statistical analysis of rotary friction welding of steel with varying carbon in workpieces

Nirmal S. Kalsi · Vishal S. Sharma

Received: 4 August 2009 / Accepted: 25 April 2011 / Published online: 12 May 2011

Abstract Nowadays, friction-welding method is accepted in many industries, particularly for joining dissimilar materials as a mass production process. It is due to advantages like less material waste, low production time, and low energy expenditure in it. The effect of change in carbon contents in steel is studied experimentally in friction-welding process and a statistical model is developed. An experimental setup was designed and produced to achieve the process with equal diameter workpieces. Continuous/direct drive friction-welding process is chosen in which transition from friction to forging stage can be achieved automatically by applying a brake. In this experimentation, workpieces with different carbon in each were welded with workpieces having same carbon contents. Response surface methodology of design of experiment is used to analyze the results. Friction welding is carried out with change of speed, forging pressure, and carbon content while keeping other parameters as constant. Tensile strength and hardness variations were obtained and examined in the post-weld at the joint of workpieces. The optimum welding parameters for the joints were obtained. Mathematical equations in terms of each output parameter are then validated experimentally.

Keywords Friction welding · Percentage of carbon in steel · Tensile strength · Hardness

N. S. Kalsi (✉)
Department of Mechanical Engineering,
Beant College of Engineering & Technology,
Gurdaspur, Punjab, India
e-mail: ns_kalsi@yahoo.com

V. S. Sharma
Department of Industrial & Production Engineering,
National Institute of Technology,
Jalandhar, Punjab, India

1 Introduction

Since the friction-welding process produces full face homogeneous joints, it is accepted as an extremely reliable in production process. It has wide number of applications in automobile, nuclear, aerospace, electrical, chemical, cryogenic, marine, etc. Friction welding is getting higher state among other welding methods due to most economical, highly productive, and clean and dry method of joining different metals and alloys [1]. The process is used to weld most grades of the ferrous materials and, in addition, has the proven ability to join widely different combinations of non-ferrous materials such as copper to aluminum, copper to steel, stainless steel to aluminum, etc. Friction welding is acceptable for reducing the costs of complex forgings or castings, e.g., welding of spindle/shaft to casted/forged head, etc. The process can be used to join metals of widely differing mechanical and thermal properties. Often, combinations that can be friction welded cannot be joined by other welding techniques [2].

In this process, heat is generated by conversion of mechanical energy into thermal energy due to friction, at the interface of the workpieces during rotation under pressure against another one [3]. The developed heat at the interface raises the temperature of workpieces rapidly, over a short axial distances, to the values approaching the melting range of the material. Welding occurs under the influence of pressure that is applied when heated zone is in the plastic range [4]. Savings in material can also be realized by the use of friction welding, especially when joining large diameter rotor bodies/other rounded parts or joining the components of valve systems [5]. The problem comes not only from the different melting points and hardness of the dissimilar materials to be joined, but also from the possibility of either brittle intermetallic com-

pounds or low melting point eutectics at the interface. In aluminum–steel welding, intermetallic compounds are a major problem. These intermetallic compounds are undesirable. Dawes [6] introduced a relationship between the properties of material forming brittle intermetallic compounds and the time available for the formation of the compounds. He concluded that the satisfactory welds could be made by keeping incubation period longer than the welding time. However, the existence of an incubation period for intermetallic formation is questionable. So, the control should be based on limiting the thickness of intermetallic rather than on using an incubation period [7]. The process can be described best in the four stages as shown in Fig. 1.

Generally, rotary friction welding process can be classified in two as continuous/direct drive friction welding and inertia/stored energy friction welding [8]. In continuous drive friction welding, which is also known as direct drive friction welding, heat is generated at the joint by rotating one part against another at a constant or varying speed, with an axial pressure applied between the mating parts. Energy is provided from a continuously running prime mover, usually an electric motor which is directly connected to the machine spindle. This energy source is infinite with respect to time, and energy is supplied to the interface until proper heat is generated. When this state reaches, the rotating component is stopped quickly while the axial pressure, known as forging pressure at this stage, is increased for a predetermined time. Graphical representation of the process is as shown in Fig. 2.

Various researchers such as Vill [9] and Tylecote [10] investigated the parameters that influence the welding quality, strength of the joint, and hardness of the heat-affected zone (HAZ). Dobrovidov et al. [11] investigated the selection of optimum conditions for the friction welding

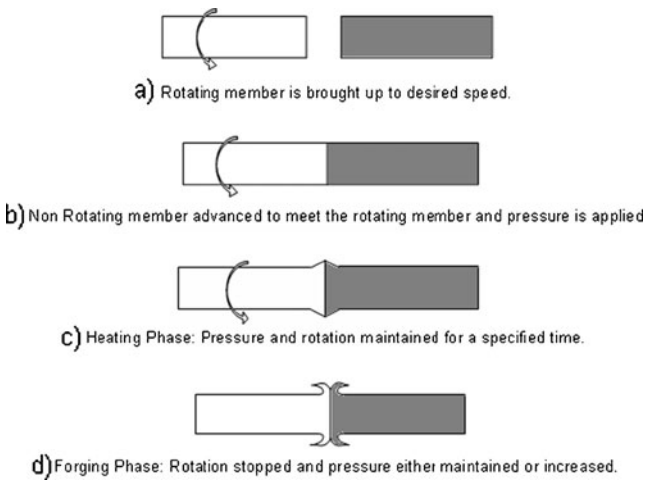

Fig. 1 Stages of friction welding process (**a**, **b**, **c**, **d**)

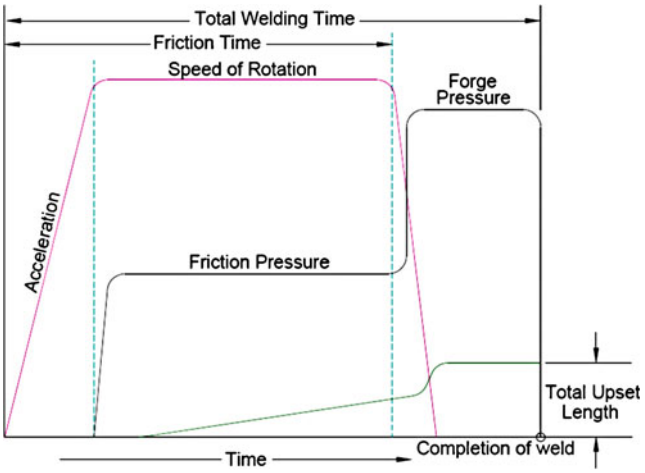

Fig. 2 Graphical presentation of the process

of high-speed steel R6M5 to carbon steel 45. Sahin et al. [8, 12] examined the tensile strength, hardness of the HAZ, fatigue strength, notch-impact strength, and microstructure of weld with high-speed steel (HSS-S 6-5-2) and medium carbon steel (AISI 1040). Sketchley et al. [13] investigated microstructure and studied mechanical properties. They demonstrated that the Fe3Al–ODS alloy can be joined easily to itself and Haynes 230 alloy using continuous drive rotary friction welding, regardless of the metallurgical condition of the alloy. Optimum parameters were obtained to join AISI 1040 parts having equal diameter and then effects of welding parameters on welding strength and mechanical properties of joints were examined by using tensile tests, fatigue tests, notch-impact tests, and hardness tests [12]. Sahin and Akata [14] investigated friction welding of plastically deformed steels for their tensile strength and variation of hardness near the joint by applying a statistical technique. Zdemir and Orhan [15] examined microstructure and mechanical properties of friction-welded joints of a fine-grained hypereutectoid steel with 4% Al. D'Alvise et al. [16] developed the finite element model of the inertia friction-welding process between dissimilar materials and established the results related to common parameters.

Then, Sahin and Akata [17] investigated welding quality using tensile test of the welded parts that have different cross-sections. Akata et al. [18] conducted a detailed study on the friction-welding setup. Sahin and Akata [19] made an investigation on friction welding of medium carbon steel and austenitic stainless steel. Yoon et al. [20] studied the mechanical properties of friction welds of RAFs (JLF-1) to SUS304 steels as measured by the acoustic emission technique and was confirmed experimentally that real-time quality evaluation of a weld was possible by acoustic emission technique. The tests were tensile tests and Vickers hardness surveys of the bond of area and HAZ. Sahin [21]

has also simulated friction welding using a computer program for AISI 1040 (medium carbon steel). For most metals, the strength of a friction-welding joint is about the same as that of the base metal in case of friction welding between similar metals [22]. But in case of friction welding between dissimilar metals, the strength may be up to 75% of the strength of the weaker metals. Zimmerman et al. [23] modeled friction welding of elastic materials with elastic–plastic metals. This model has been practically verified in the process of friction welding of corundum ceramic of 97.5% Al_2O_3 content and aluminum alloy 6061-T6 as well as in the same ceramic and electrolytic copper of 99.9% Cu content. Finite element simulation was used to make it possible to observe the temperature distribution and thermo-mechanical fields that take place during the process. Results show that the temperature, pressure, and deformation distribution near the contact surface are non-homogeneous. Luo et al. [4] analyzed the macrostructure of welding flashes and friction weld results have shown that proposed mixed-integrated approach eliminates the problem of the flashes in the damping-tube friction welding. A comparative thermal analysis of the friction welding process using various heat generation models is made. The heat generation rate in orbital friction welding of steel bars is analyzed using four different methods: constant coulomb friction, sliding–sticking friction, the experimentally measured power data, and an inverse heat conduction approach.

In spite of long tradition of industrial use of this welding process, there is much to know about the process. The aim of this paper is to find out the effect of carbon particles present in the workpiece material due to its importance in almost every type of steel.

2 Experimental setup

Conventional friction-welding apparatus resembling a HMT LB-17 lathe machine was selected. Its specifications are: speed range 45 to 2,000 rpm, number of speed steps 18, motor 7.5 kW, distance between centers 1 m, and height of center 170 mm. Ancillary equipment for applying axial pressure during welding is designed and fitted separately by modifying the tail stoke. A pressure gauge (range 0–350 Kgf/cm^2) was mounted to indicate axial pressure applied. To carry out welding, the workpiece in the chuck was rotating and brought in contact with stationary specimen, held in special fixture. Experimental setup used for this experiment is as shown in Fig. 3. The heating pressure was applied and maintained till the melting point of the workpiece is reached. The machine rotation was then stopped suddenly and finally forge pressure was applied.

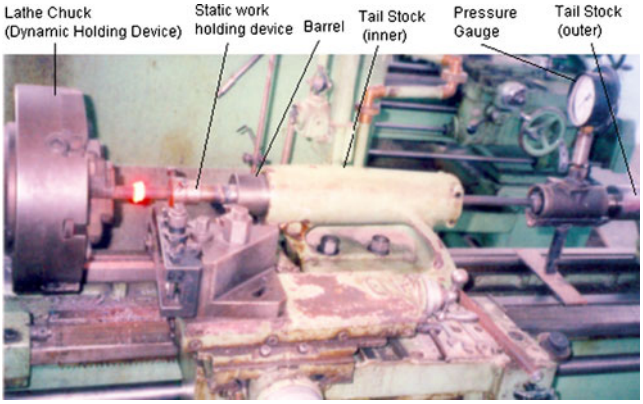

Fig. 3 Experimental setup

3 Selection of material

Material selection is based upon the carbon value in it. Different grades of the carbon steel are selected, whose carbon value is varying keeping other contents almost same. Standard values are as shown in the Table 1. Actual values are tabulated after chemical analysis of the material. Materials are selected with different carbon values neglecting minor variations or negligible presence of other foreign compounds in it.

4 Process parameters

The input process parameters in friction-welding process may be as: rotational speed, friction pressure, forging pressure, heating time, forging time, contents of the steel, melting point of the material, thermal conductivity of the material, diameter of the workpiece, surrounding temperature, thickness of oxide layer on contact surfaces, etc. A statistical approach based upon one factor at a time being tedious and much time consuming, statistical design of experiment based response surface methodology is selected to analyze the process, where a response surfaces are generated for each response under consideration. Keeping in view the importance of rotational speed and forging pressure [7, 24] both parameters along with change in carbon contents, which has not been found evaluated earlier, is considered for analysis.

The output parameters are tensile strength, rise in hardness of the workpiece, upset (decrease in length of the workpiece), bending strength, change in lateral dimensions, other mechanical/chemical properties and structural changes, etc. Important parameters, tensile strength and increase in hardness of the joint in final weld, have been analyzed to develop a statistical model and then the model is validated with actual practical values.

Table 1 Standard and actual composition of selected materials

S. no.	Grade		% C	% Mn	% S	% P	% Si	% Cr	% Ni	% Mo
1	C14	Std.	0.10–0.18	0.40–0.70	0.035	0.035	0.10–0.35	–	–	–
		Actual	0.11	0.51	0.036	0.035	0.2	–	0.005	0.003
2	CLIA	Std.	0.10–0.20	0.60–0.90	0.035	0.035	0.15–0.30	–	–	–
		Actual	0.13	0.52	0.035	0.037	0.19	0.01	0.015	–
3	C35	Std.	0.32–0.39	0.50–0.80	0.035	0.035	0.15–0.35	–	–	–
		Actual	0.37	0.53	0.035	0.036	0.2	–	0.01	–
4	C55	Std.	0.50–0.55	0.60–0.80	0.04	0.04	0.15–0.30	–	–	–
		Actual	0.52	0.51	0.036	0.035	0.19	–	0.01	0.002
5	C60	Std.	0.57–0.65	0.60–0.90	0.035	0.035	0.15–0.30	–	–	–
		Actual	0.64	0.52	0.035	0.035	0.18	–	–	0.005

Std. standard, *C* carbon, *Mn* manganese, *S* sulfur, *P* phosphorous, *Si* silicon, *Cr* chromium, *Ni* nickel, *Mo* molybdenum

A preliminary step in any experiment of this type is to decide the lower and upper limit of the process parameters. The input parameters with their working range and output parameters are as mentioned in the Tables 2 and 3. The experiments have been conducted as per the Appendix 1.

5 Experimental procedure

The specimens of carbon steels and mild steels were first cut to the length of about 250 mm on an automatic hacksaw machine. This length was kept leaving about 2 mm margin for facing operation on the Lathe machine later, before the process. After facing, these were thoroughly cleaned with detergent, washed with clean water, and finally dried.

Once the specimens were ready for experimental purpose, carbon steel and mild steel workpieces were taken one by one by holding carbon steel workpiece in the chuck of the lathe machine which is also known as dynamic holding device and the mild steel workpiece was held in the static holding device (special fixture). The machine then was set for its rotational speed as per set of designed value and started which is then measured with help of digital tachometer. Axial movement was then given to mild steel workpiece till both the pieces come in contact with each other. Axial heating pressure was then applied for 20 s, till the pieces were heated to the red. Rotation was then stopped instantly by pressing the stop pedal of machine with application of brake and finally forge pressure was applied for 15 s, which is comparatively more than the heating pressure as per set of design values. The time to weld was noted with help of digital watch capable of reading up to microsecond. Workpiece is then taken out. Flange, which is formed during welding process then machined by holding the workpiece in the chuck of another lathe machine of the similar type. Finally, prepared specimens were then taken to measure tensile strength and increase in hardness in the vicinity of the joint. Corresponding readings were tabulated in the required format as shown in Appendix 1.

6 Tensile strength

The data presented in the Appendix 1 are analyzed for tensile strength. An analysis of variance (ANOVA) is conducted. The objective is to determine which factors and factor interactions are statistically significant in affecting the tensile strength. ANOVA for tensile strength parameters is as shown in Table 4. This table indicates sum of squares, degrees of freedom (*df*), mean square (MS), *F* value, and *p* value associate with each factor level and interaction. The ANOVA table also indicates the significance of the model obtained.

The model *F* value of 11.4461 implies that the model is significant. There is only 0.03% chance that "Model *F* Value" this large could occur due to noise. Values of "Prob>*F*" less than 0.0500 indicate model terms are significant. In this case, A, B, and C are significant model terms. The "Lack of Fit *F* value" of 195.96 implies the lack of fit is significant. There is only 0.01% chance that "Lack of Fit *F* value" this large could

Table 2 Input parameters

	Factor, X_s	Units	Low level	High level
A	Speed (*S*)	rpm	810	1,620
B	Forging pressure (FP)	Kgf/cm^2	40	80
C	Carbon (*C*)	Percentage	0.13	0.52

Table 3 Output parameters

S. no.	Responses, Y_s	Units
01	Tensile Strength (*T*)	Kg/cm^2
02	Hardness (*H*)	HRB

HRB Rockwell B hardness

Table 4 ANOVA table for tensile strength

Source	Sum of squares	*df*	Mean square (MS)	*F* value	Prob>*F*
Model	7,086,545	3	2,362,182	11.4461	0.0003
A	2,088,868	1	2,088,868	10.12175	0.0058
B	2,037,638	1	2,037,638	9.873506	0.0063
C	2,923,335	1	2,923,335	14.16521	0.0017
Residual	3,301,989	16	206,374.3		
Lack of fit	3,294,348	11	299,486.1	195.9603	<0.0001
Pure error	7641.5	5	1,528.3		
Cor total	10,388,535	19			
Std. Dev.	454.2844	R-squared	0.682151		
Mean	7382.35	Adj R-squared	0.622554		
C.V.	6.153656	Pred R-squared	0.477034		
PRESS	5,432,847	Adeq precision	12.65784		

Std. Dev. standard deviation, *df* degrees of freedom

occur due to noise. The "Pred R-Squared" of 0.4770 is in reasonable agreement with the "Adj R-Squared" of 0.6226. "Adeq Precision" measures the signal-to-noise ratio. A ratio greater than 4 is desirable. The ratio of 12.658 indicates an adequate signal. The regression equation obtained for tensile strength in terms of input parameter is as follows:

$$\text{Tensile strength} = 4{,}094.75 + 0.99\,S + 19.35\,\text{FP} + 2{,}535.43\,C \quad (1)$$

This resultant regression (Eq. 1) shows the dependence of tensile strength on all three input parameters, i.e., speed, forging pressure, and carbon content in the workpieces during the process. Then, surface plots can be generated for the tensile strength versus two of the variables at a time. In this case, there are three variables so there are three surface plots (Figs. 4, 5, and 6). For each of the plots, the variable not represented is held at a constant value and is as mentioned. These graphs allow to qualitatively find a minimum or maximum for the tensile strength. The behavior of each parameter relative to other can be observed from surface plots. It clearly indicates that the value of tensile strength increases gradually with respect to all the three input variables, i.e., speed, forging pressure, and carbon contents in the material and maximum tensile strength can be achieved by keeping all the three variables at the high in this range. Figure 7 represents a plot that indicates the effect of all variables on tensile strength. This clearly indicates that the tensile strength is affected by all the three variables and behavior is almost similar.

6.1 Validation of the results

To check the validation of this experiment and the equation, the study of tensile strength as an output

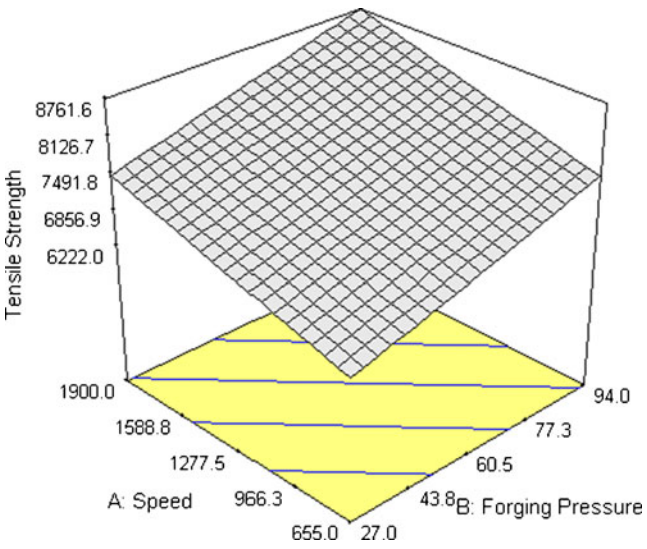

Fig. 4 Tensile strength vs. forging pressure and speed, carbon %=0.37 (constant)

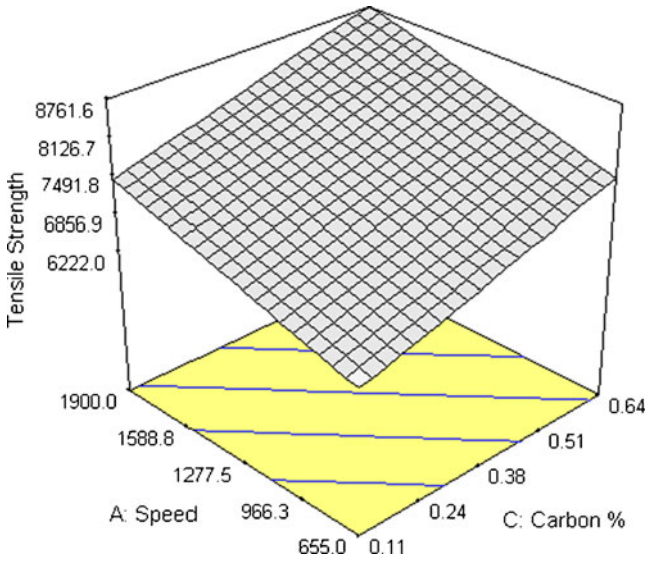

Fig. 5 Tensile strength vs. carbon and speed, forging pressure= 60.5 kgf/cm^2 (constant)

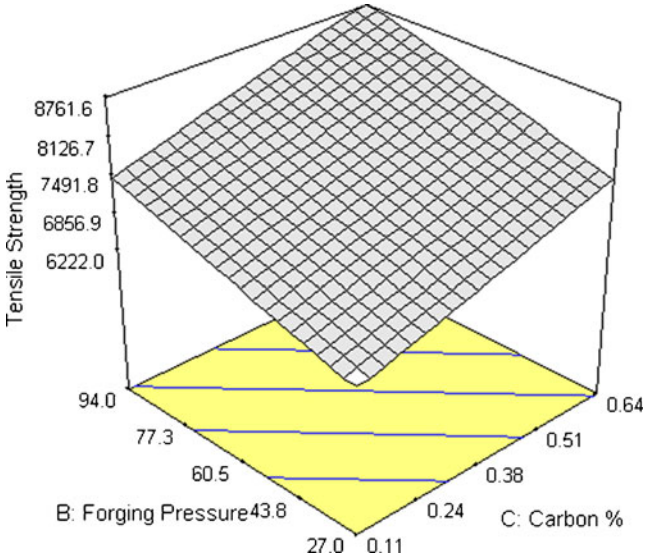

Fig. 6 Tensile strength vs. carbon and forging pressure, speed= 1275 rpm (constant)

parameter is done relative to the speed variation by keeping carbon contents and forging pressure constant. Figure 8 shows the behavior of change in tensile strength value by using mathematical Eq. 1 and by conducting the experiments. It is very clear that values are almost same as both the bars are very close to each other. The average error is very small, i.e., 3.19% (Appendix 2). Therefore, we can say that expression in terms of tensile strength value is a valid expression.

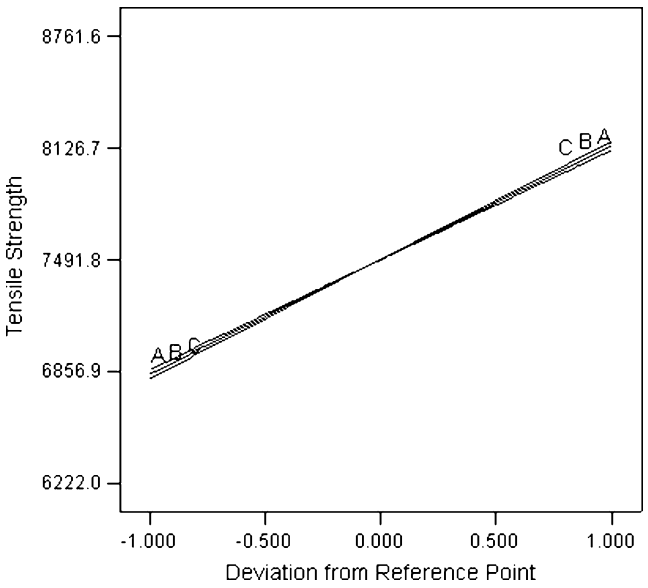

Fig. 7 Overall effects of variables on tensile strength

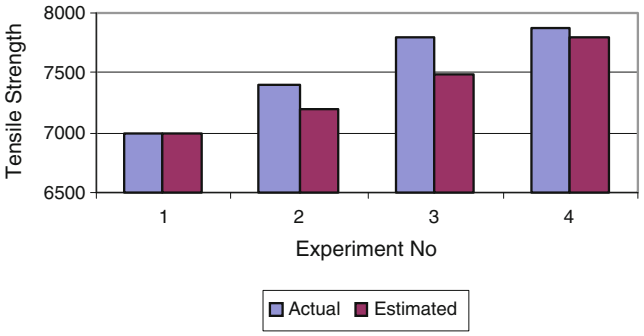

Fig. 8 Estimated and actual behavior of tensile strength

7 Increase in hardness

Hardness is measured near the joint up to 5 mm distance from the interface of the joint in the heat-affected zone. Both base specimen and welded specimen are considered to measure the hardness value. Observations in this respect are tabulated which are shown in Table 5. Where zero indicates the center of the joints and hardness value is noted up to 5 mm with an interval of 1 mm. It is measured on HRB scale.

Values for each specimen as tabulated graphically are shown in Fig. 9. The drop in hardness close to the interface indicates decarburisation of high carbon material, although it increases a little very close to the joint due of hardening effect, which is always more in the case of high carbon material. The heat-affected zone is of maximum 5 mm and beyond this the hardness becomes equal to the hardness of the actual material. It is very clear from the trends that with the increase of carbon content of the material, the hardness increases in the heat-affected zone. This also partially depends upon applied forging pressure. Ultimately, a change in hardness in the heat-affected zone is higher when carbon in the material is high, and it also increases with increasing values of forging pressure.

7.1 Analysis for increase in hardness

The data in the Appendix 1 were analyzed for "Increase in Hardness" and ANOVA is formulated as Table 6. The model F value of 56.87 implies that the model is significant. There is only 0.01% chance that "Model F Value" this large could occur due to noise. The values of "Prob>F" less than 0.0500 indicate model terms are significant. In this case, factor A does not seem to be significant, whereas B and C are significant model terms. The "Lack of Fit F value" of 3.31 implies there is 9.84% chance that "Lack of Fit F value" this large could occur due to noise. The "Pred R-Squared" of 0.8717 is in reasonable agreement with the "Adj R-Squared" of 0.8982. "Adeq

Table 5 Hardness value in the vicinity of the joint

		Runs	Hardness, HRB																			
			1	2	3	4	5	6	7	8	9	10	11	12	13	14	15	16	17	18	19	20
Distance from center, mm	Welded material	5	64	74	69	70	69	65	70	66	65	69	66	75	70	69	68	69	75	69	74	78
		4	65	76	71	71	70	66	72	67	67	70	66	77	72	70	69	71	76	70	75	79
		3	65	77	74	72	71	66	73	67	67	71	67	78	72	70	72	70	77	70	75	81
		2	66	82	76	74	75	67	75	68	68	72	67	79	73	73	73	72	78	72	79	83
		1	66	87	77	75	77	68	78	68	69	76	68	84	79	76	76	73	81	77	82	88
		0	67	83	75	74	76	68	76	70	69	76	68	82	76	73	74	72	78	74	77	85
	Base material	−1	67	76	73	70	71	68	70	68	68	70	67	78	70	69	69	67	74	69	73	81
		−2	66	73	68	67	68	67	69	68	67	69	66	70	68	68	67	67	71	69	70	78
		−3	66	69	68	66	68	68	68	67	67	67	65	67	66	68	66	66	68	67	68	72
		−4	65	67	66	65	66	66	66	67	65	66	66	65	67	67	66	66	68	67	67	69
		−5	65	66	65	65	65	66	67	65	65	66	66	66	65	67	65	65	66	66	65	67

HRB Rockwell B hardness

Precision" measures the signal-to-noise ratio. A ratio greater than 4 is desirable. The ratio of 23.954 indicates an adequate signal. It shows that the model is significant. The regression equation obtained for increase in hardness in terms of input parameter is as follows:

$$\text{Increase in hardness} = -2.64 + 5.08E - 004\ S + 0.06\ \text{FP} + 14.81\ C \quad (2)$$

This resultant regression (Eq. 2) shows the dependence of increase in hardness on all three input parameters, i.e., speed, forging pressure, and carbon content in the workpieces during the process. Then surface plots are generated for the increase in hardness versus two of the variables at a time. In this case, there are three variables so there are three surface plots (Figs. 10, 11, and 12). For each of the plots, the variable not represented is held at a constant value and the value is as shown. These graphs allow to qualitatively find a minimum or maximum for the increase in hardness. An increase in hardness with respect to forging pressure can be observed in Fig. 10, is increasing gradually whereas speed does not show much significant effect. Change in carbon contents shows a significant impact on increase in

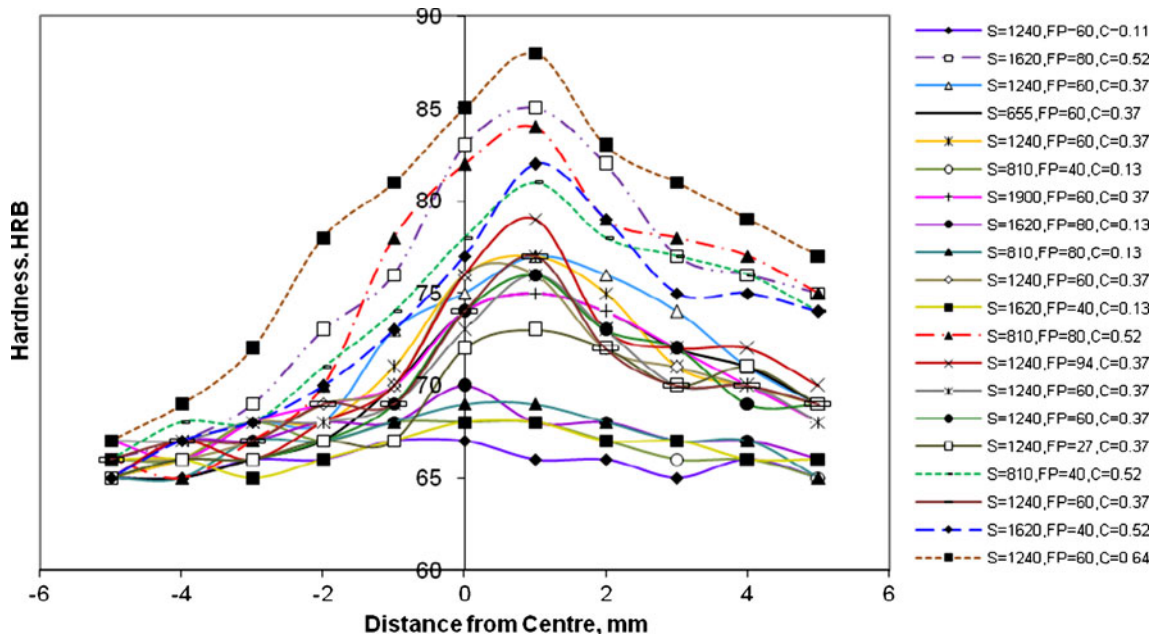

Fig. 9 Hardness variations in specimens

Table 6 ANOVA table for increase in hardness

Source	Sum of squares	*df*	Mean square (MS)	*F* value	Prob>*F*
Model	117.7559	3	39.25196	56.86561	<0.0001
A	0.540294	1	0.540294	0.782742	0.3894
B	17.32496	1	17.32496	25.09924	0.0001
C	99.75362	1	99.75362	144.5164	<0.0001
Residual	11.04413	16	0.690258		
Lack of fit	9.710799	11	0.8828	3.310499	0.0984
Pure error	1.333333	5	0.266667		
Cor total	128.8	19			
Std. Dev.	0.830818	R-squared	0.914254		
Mean	6.6	Adj R-squared	0.898176		
C.V.	12.58815	Pred R-squared	0.871699		
PRESS	16.52517	Adeq precision	23.95363		

Std. Dev. standard deviation, *df* degrees of freedom

hardness in a particular range as shown in Fig. 11, whereas for very small and very high carbon content does not give drastic variation in increase in hardness which may be due that a very small quantity of carbon in the material shall not be able to participate to improve the hardness to much extent and a very excessive carbon shall be in the form of free carbon and will not be able to improve the hardness further. Similarly, it can be observed from Fig. 12 that both carbon contents and forging pressure contribute to an increase in hardness and the behavior at different ranges are as shown. Figure 13 represents a plot that indicates the effect of all variables on increase in hardness. This clearly indicates that the increase in hardness is affected by all the three variables and the impact of carbon content is the highest followed by forging pressure and then by speed during the process.

7.2 Validation of the results

Variation in "Increase in Hardness" with change in input parameters—carbon contents, forging pressure, and relative speed is analyzed and Eq. 2 is formulated. To check the validation of this equation experimentally, the study is done relative to speed variation by keeping carbon contents and forging pressure constant. Figure 14 shows the behavior of increase in hardness by using mathematical Eq. 2 and by conducting the experiments. It represents an average error of 7.39 % and a maximum of 10.164 % (Appendix 2) for increase in hardness. Using predicted mathematical equation for increase in hardness, actual hardness value was calculated as 75.6361, 75.7377, 75.89 and 76.0424 HRB whereas hardness after experimentation was 76, 77, 77 and 77 HRB for validation experiment no. 1, 2, 3 and 4 respectively.

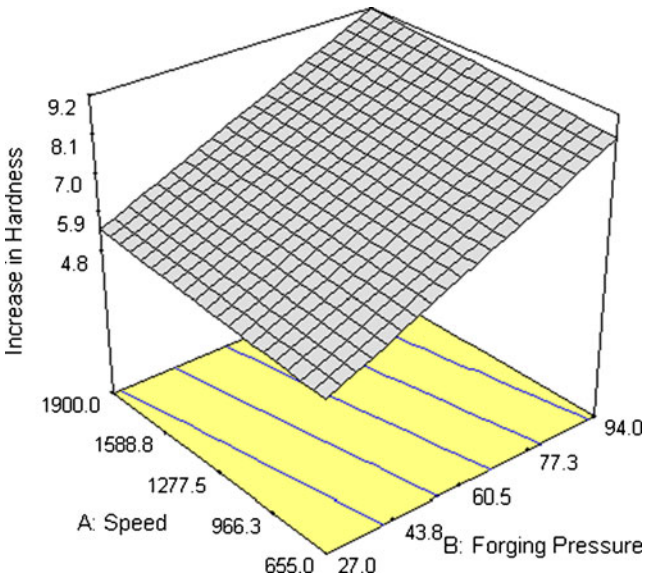

Fig. 10 Increase in hardness vs. forging pressure and speed, carbon %= 0.37 (constant)

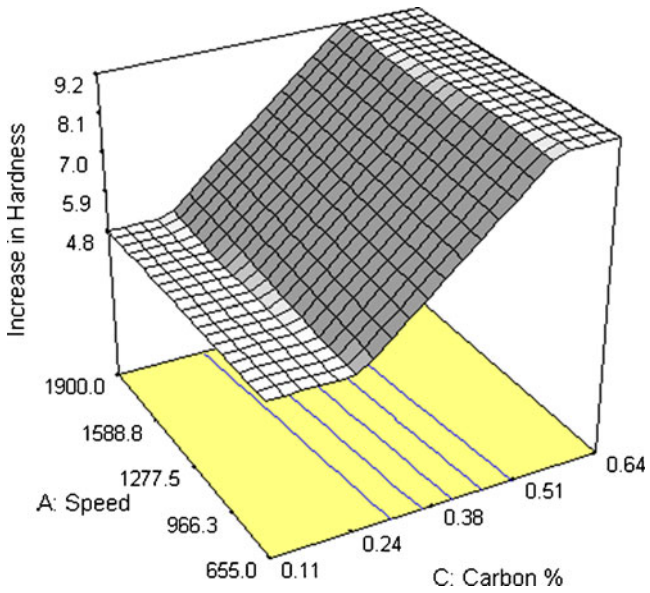

Fig. 11 Increase in hardness vs. carbon and speed, forging pressure= 60.5 kgf/cm^2 (constant)

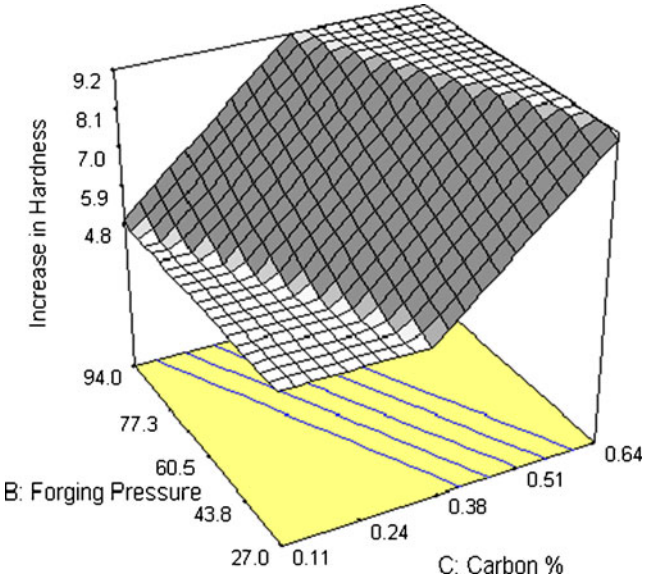

Fig. 12 Increase in hardness vs. carbon and forging pressure, speed= 1275 rpm (constant)

This gave a maximum error of 1.64 % in prediction of final hardness value in the workpiece, which in negligible. This change may be due to a change in initial setup, rigidity of the machine, repeatability of the forging pressure, environmental factors, or change in standard conditions, etc. and some time uncontrollable. Hence, validation of the equation is confirmed.

8 Optimization

To optimize these experimental results, the output parameters, i.e., increase in harness is minimized and tensile strength is maximized. The results are indicated in

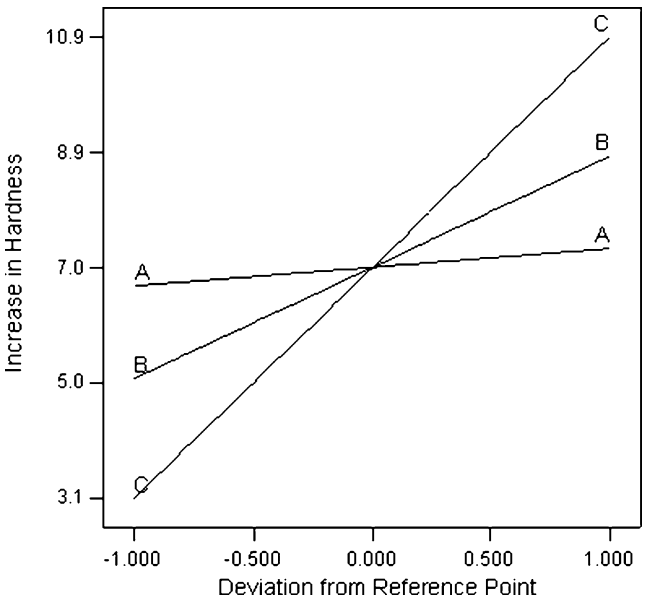

Fig. 13 Overall effects of variables on increase in hardness

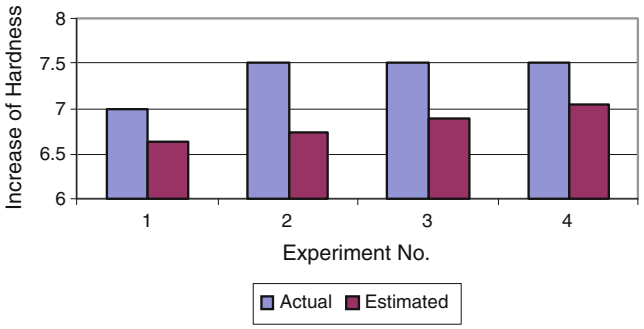

Fig. 14 Estimated and actual values of increase in hardness

Table 7. The speed of 1,620 rpm, forging pressure of 79.99 Kgf/cm^2, and carbon contents of 0.13% would give the best result in this design to develop maximum tensile strength and minimum increase in hardness. The maximum desirability that can be achieved in this design is 0.789.

9 Conclusions

The major conclusions drawn out of the study are:

1. Speed, forging pressure, and carbon content have significant affects on tensile strength of the joint. It increases gradually with the increase in values of the parameters.
2. Both forging pressure and carbon content in the specimens play a major role in increase in hardness of the final weld, whereas carbon content affects it more as compared to forging pressure.
3. Very low carbon in the material up to 0.2% and 0.6% or above do not give a significant change in hardness.
4. At very low values of carbon, an increase in forging pressure increases the hardness value.
5. With optimum parameters, more than 100% tensile strength of the welded joint can be achieved as of the specimen of weaker material.

Table 7 Optimized value of the parameters with desirability

Number	Speed	Forging pressure	Carbon content	Tensile strength	Increase in hardness	Desirability
1	1,620	79.99	0.13	7,589.66	4.63	0.789
2	1,620	79.82	0.13	7,586.53	4.62	0.789
3	1,620	79.53	0.13	7,580.79	4.60	0.789
4	1,620	78.36	0.13	7,558.18	4.53	0.789
5	1,620	77.86	0.13	7,548.62	4.51	0.788

6. The proposed Eqs. 1 and 2 for the tensile strength and increase in hardness, respectively, shall be able to predict the parameters with high accuracy for this setup.

Table 8 Experimental design

Run no.	Speed (*S*), rpm	Forging pressure (FP), Kgf/cm^2	Carbon (*C*),%	Tensile strength, Kg/cm^2	Increase hardness, HRB
1	1,240	60	0.11	6,317	2
2	1,620	80	0.52	7,889	10
3	1,240	60	0.37	7,806	8
4	655	60	0.37	6,139	6
5	1,240	60	0.37	7,783	8
6	810	40	0.13	5,431	3
7	1,900	60	0.37	7,839	7
8	1,620	80	0.13	7,833	4
9	810	80	0.13	7,083	4
10	1,240	60	0.37	7,722	7
11	1,620	40	0.13	7,039	2
12	810	80	0.52	7,833	9
13	1,240	94	0.37	7,861	9
14	1,240	60	0.37	7,806	8
15	1,240	60	0.37	7,833	7
16	1,240	27	0.37	6,333	4
17	810	40	0.52	7,611	7
18	1,240	60	0.37	7,817	8
19	1,620	40	0.52	7,833	8
20	1,240	60	0.64	7,839	11

Appendix 1

Table 9 Validation experiments

S. no.	Speed, rpm	Increase in hardness, HRB (actual)	Increase in hardness, HRB (estimated)	% error
01	800	7	6.6361	5.198571
02	1,000	7.5	6.7377	10.164
03	1,300	7.5	6.8900	8.133333
04	1,600	7.5	7.0424	6.101333
S. No.	Speed, rpm	Tensile strength, Kg/cm^2 (actual)	Tensile strength, Kg/cm^2 (estimated)	% error
01	800	7,000	6.9925e+003	0.107143
02	1,000	7,400	7.1923e+003	2.806757
03	1,300	7,800	7.4919e+003	3.95
04	1,600	7,880	7.7915e+003	1.123096

Carbon percentage 0.37% (constant), forging pressure 60 Kgf/cm^2 (constant)

C carbon percentage, *FP* forging pressure, *HRB* Rockwell B hardness

Appendix 2

References

1. Jessop TJ, Dinsdale WO (1978) Friction welding dissimilar metals. Proc. Conf. Advances in Welding Processes, Harrogate, The Welding Institute, 49
2. Sahin AZ, Yibas BS, Ahmed M, Nickel J (1998) Analysis of the friction welding process in relation to the welding of copper and steel bars. J Mater Process Technol 82:127–136
3. Yilbas BS, Sahin AZ, Coban A, Aleem BJ (1994) Investigation into the properties of friction-welded aluminium bars. J Mater Process Technol 54:76–81
4. Luo J, Ye YH, Xu JJ, Luo JY, Chen SM, Wang XC, Liu KW (2009) A new mixed-integrated approach to control welded flashes forming process of damping-tube–gland in continuous drive friction welding. Mater Des 30:353–358
5. Black RA (1983) Friction welding cryogenic components for the JET project. Met Constr 15(574):576
6. Dawes CJ (1977) Micro-friction welding aluminium studs to mild steel plates. Met Constr 9:196–197
7. Yilbas BS, Sahin AZ, Kahraman N, Al-Garni AZ (1995) Friction welding of St-A1 and A1-Cu materials. J Mater Process Technol 49:431–443
8. Sahin M (2005) Joining with friction welding of high-speed steel and medium-carbon steel. J Mater Process Technol 168:202–210
9. Vill VI (1962) Friction welding of metals. AWS, New York, 1962
10. Tylecote RY (1968) The solid phase welding of metals. Arnold, London, pp 1–50
11. Dobrovidov AN et al (1975) Selection of optimum conditions for the friction welding of high-speed steel 45. Weld Prod 22:22–26
12. Sahin M, Akata HE, Gulmez T (2007) Characterization of mechanical properties in AISI 1040 parts welded by friction welding. Mater Charact 58:1033–1038
13. Sketchley PD, Threadgill PL, Wright IG (2005) Rotary friction welding of an Fe3Al based ODS alloy. Mater Sci Eng A329–331:756–762
14. Sahin M, Akata HE (2003) Joining with friction welding of plastically deformed steel. J Mater Process Technol 142:239–246
15. Zdemir NO, Orhan N (2005) Microstructure and mechanical properties of friction welded joints of a fine-grained hypereutectoid steel with 4% Al. J Mater Process Technol 166:63–70
16. D'Alvise L, Massoni E, Walloe SJ (2002) Finite element modelling of the inertia friction welding process between dissimilar materials. J Mater Process Technol 125(126):387–391
17. Sahin M, Akata HE (2002) An investigation on friction welding of AISI 1040 and AISI 304 steels, in: Proceedings of ESDA 2002. Sixth Biennial Conference on Engineering Systems Design and Analysis, 8–11 July, Istanbul, Turkey
18. Akata E, Sahin M, Becenen I (2001) Application of some automatic control circuits to an experimental friction welding set-up, in: Second Annual Conference with International Participation on Rapid Technologies One More Line Allowed End, 14–15 November, Stellenbosch, South Africa
19. Sahin M, Akata HE (2001) An experimental study on application of friction welding for parts with different diameters and width.

The Third International Congress Mechanical Engineering Technologies 01, 24–26 June, Sofia, Bulgaria
20. Yoon HK, Kong YS, Kimb SJ, Kohyama A (2006) Mechanical properties of friction welds of RAFs (JLF-1) to SUS304 steels as measured by the acoustic emission technique. Fusion Eng Des 81:945–950
21. Sahin M (2004) Simulation of friction welding using a developed computer program. J Mater Process Technol 153 (154):1011–1018
22. Hascalik A, Orhan N (2005) Effect of particle size on the friction welding of Al2O3 reinforced 6160 Al alloy composite and SAE 1020 steel. Mater Des 28:313–317
23. Zimmerman J, Wlosinski W, Lindemann ZR (2009) Thermo-mechanical and diffusion modelling in the process of ceramic–metal friction welding. J Mater Process Technol 209:1644–1653
24. Murti KGK, Surdaresan S (1983) Parameter optimization in friction welding dissimilar materials. Met Constr 15:331–335